

Available online at www.sciencedirect.com

ScienceDirect

www.elsevier.com/locate/jes

JES
JOURNAL OF
ENVIRONMENTAL
SCIENCES
www.jesc.ac.cn

Contribution of the Kodama and 4S pathways to the dibenzothiophene biodegradation in different coastal wetlands under different C/N ratios

Lei Wang, Guodong Ji*, Siqiao Huang

Key Laboratory of Water and Sediment Sciences, Ministry of Education, Department of Environmental Engineering, Peking University, Beijing 100871, China. E-mail: wangleienviro@pku.edu.cn

ARTICLE INFO

Article history:

Received 8 January 2018

Revised 23 April 2018

Accepted 28 April 2018

Available online 8 May 2018

Keywords:

Dibenzothiophene (DBT)

Coastal wetlands

Functional genes

Degradation mechanism

Quantitative response relationship

Network analysis

ABSTRACT

Dibenzothiophene (DBT) degradation mechanisms and the transformation of pathways during the incubation of three types of coastal sediments with C/N ratios ranging from 1 to 9 were investigated. The DBT degradation efficiencies were clearly improved with increasing C/N ratio in reed wetland sediments, tidal wetlands sediments and estuary wetland sediments. The quantitative response relationships between DBT degradation rates and related functional genes demonstrate that the Kodama pathway-related gene groups were dominant factors at low C/N ratios, while the 4S-related gene groups mainly determined the degradation rate when the C/N ratio was up to 5. Network analysis also shows that the pathway shifts from the Kodama pathway to the 4S pathway occurred through changes in the connections between functional genomes and rates. Furthermore, there were competition and collaboration between the Kodama and 4S pathways. The 4S pathway-related bacteria were more active in estuary wetland sediments compared with reed wetland sediments and tidal wetland sediments. The higher degradation efficiency in estuary wetland sediments may indicate the greater participation of the 4S pathway in the DBT biodegradation reaction. And the effects of ring cleavage of Kodama pathway caused more complete metabolizing of DBT.

© 2018 The Research Center for Eco-Environmental Sciences, Chinese Academy of Sciences.

Published by Elsevier B.V.

Introduction

Wetlands not only consist of different habitats but also perform a wide range of stabilizing and purification functions on earth. Coastal wetlands comprise the region where land and ocean meet and their interaction is intensive. The Bohai Rim region, located in the northeast part of China, has become one of the three most densely populated and developed zones in China (Hu et al., 2010) and accounts for 25% of the Chinese GDP (Jie et al., 2015). The Bohai Rim wetlands have irreplaceable ecological functions such as nutrient cycling, regulating the

environment and maintaining biodiversity (Cheng and Zhaoyin, 2003). Due to the exploitation of oil and fuel combustion as an energy source, large volumes of domestic and industrial wastes and even oil spills have discharged into the Bohai wetlands (Hu et al., 2013; Jiao et al., 2014), with nitrogen, phosphorus, petroleum hydrocarbons and heavy metals being regarded as the main pollutant factors. As accounting for 11%–37% of sulfur content in oil (Oldfield et al., 1997), Dibenzothiophene (DBT) is very common in the seawater and coastal wetlands in the Bohai Rim (Li et al., 2006). The water of the Bohai Sea has quite a low self-cleaning ability due to its

* Corresponding author. E-mail: jiguodong@pku.edu.cn. (Guodong Ji).

limited exchange with the open sea (Liu and Zhu, 2014). Sedimentary microorganisms are becoming the focus of recent studies and play a critical role in the desulfurization and ultimate removal of DBT due to their selective enzyme-catalyzed reactions and economic efficiency compared with traditional physicochemical methods. Studies have revealed that the microbial degradation of DBT mainly consists of the Kodama and 4S pathways (Kodama et al., 1973; Li et al., 2008).

The Kodama pathway is a kind of metabolic pathway of DBT (Fig. 1a), in which C–C bonds are cut selectively by the corresponding enzyme. At the same time, the C–S bond is retained and converted to small molecular organic sulfides that are dissolved in the water, so S is still in the reaction products (Kodama et al., 1973). The degradation process of the Kodama pathway is similar to that of low aromatic hydrocarbons. DBT is oxidized by the initial dioxygenases and is then degraded by ring opening, isomerization and dehydrogenation to salicylate, which is the key and last product in the upper pathway. In the downstream metabolic process of DBT, salicylate is further metabolized to catechol by the catalysis of salicylate hydroxylase. Catechol is an important intermediate in the metabolic process, and in the ring cleavage reaction, catechol is catalyzed by the catechol 1,2-dioxygenase gene (*catA*) and the catechol 2,3-dioxygenase gene (*C23O*) and is converted to tricarboxylic acid (TCA) cycle intermediates that are finally completely oxidized to CO_2 and water (Kaufman et al., 1998). In the process of the Kodama pathway, the common initial dioxygenase genes (*nahAc*, *nagAc* and *nidA*), *catA* and *C23O* are detected and are regarded as potentially good targets for monitoring bacterial involvement in the ring cleavage of aromatics and the final steps in the degradation of DBT.

The 4S desulfurization pathway is the reaction in which the C–S bond of DBT is cut selectively through four key genes (*dszA*, *dszB*, *dszC* and *dszD*) which are shown in Fig. 1b DBT is catalyzed and converted to 2-hydroxybiphenyl, and S is released in the form of SO_3^{2-} (Kodama, 2008; Li et al., 2014). In the first step in the reaction of the 4S pathway, DBT is converted to dibenzothiophene sulfoxide and then to dibenzothiophene sulfone (DBTO2) by dibenzothiophene monooxidase (*dszC*). Later, DBTO2 is catalyzed by DBTO2 monooxygenase (*dszA*), and a new intermediate, 2-(2-hydroxyphenyl)-benzene sulfonate (HBPS), is produced. Finally, with the participation of the sulfonate desulfurization enzyme (*dszB*), which

plays a key role in cutting the C–S bond, HBPS is converted to 2-hydroxybiphenyl (HBP), and S is oxidized into SO_3^{2-} ; thus, sulfur is released. The enzyme *dszD* seems to be an auxiliary enzyme, participating in the entire reaction process (Abbasian et al., 2016). Because the key step of the 4S pathway is final desulfurization, the *dszB* gene can be regarded as a marker gene for the degradation of DBT.

Essentially, sedimentary microorganisms play a dominant role in the ultimate removal of DBT adsorbed on them via a series of enzyme-catalyzed reactions (Seo et al., 2009). Studies of DBT-degrading bacteria are limited to single-strain or a few microorganisms isolated from sediments. These studies scarcely involve the effect on the other non-petroleum hydrocarbon-degrading bacteria by DBT-degrading bacteria. For high-sulfur petroleum pollution in estuary and coastal wetlands, the research on the Kodama and 4S pathways of microbial desulfurization is relatively thorough. However, whether there is a corresponding relationship between the pathways and which pathway is more dominant under natural conditions need to be further studied. The recent studies of the aromatic hydrocarbon biodegradation pathways in sediments were rarely concerned about the C/N ratio, which is clearly regarded as an important factor in the directional propagation of microorganisms. Studies on the contribution and correlation of the Kodama and 4S pathways in the degradation of DBT from different coastal wetland sediments are few (Xin et al., 2017; Diao et al., 2017; Huang et al., 2013).

In this study, we choose reed wetland sediments (RWS), tidal wetland sediments (TWS) and estuary wetland sediments (EWS), culturing them for 56 days at different C/N ratios and then measuring the degradation efficiency of DBT and the abundance of functional genes. We analyze the regularity of degradation functional genes in the Bohai Rim wetland sediments and establish the response relationship between the DBT degradation rates and the functional gene groups by qPCR technology, path analysis and network analysis.

1. Materials and methods

1.1. Site description and sampling

Sediment samples were mainly collected from three wetlands on the coast of the Bohai Sea: RWS collected from the Liao

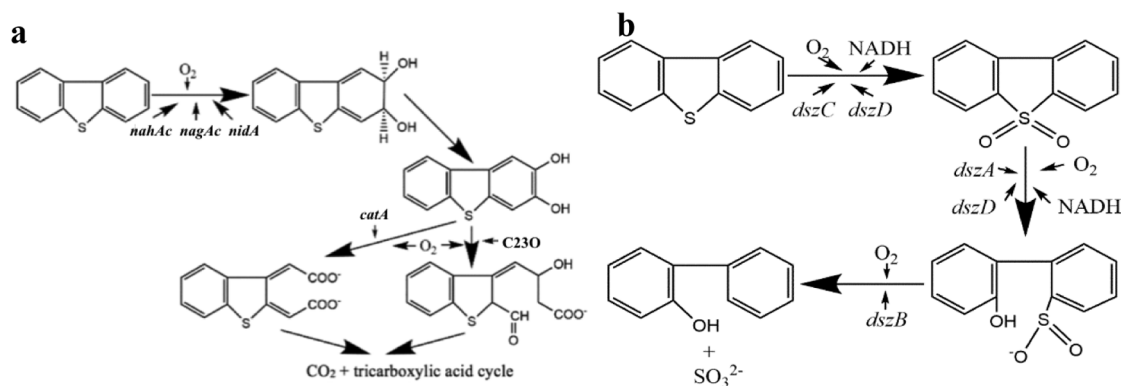


Fig. 1 – Functional genes for the degradation of DBT (Dibenzothiophene) by the Kodama pathway and the 4S pathway. (a) Kodama pathway; (b) 4S pathway.

River estuary, TWS collected from Beida harbor and EWS collected from the Yellow River estuary. The entire coast of the Bohai Sea is artificially divided into three large regions, Liaodong Bay, Bohai Bay and Laizhou Bay. The three sampling sites mentioned above are, respectively, near these three bays (Fig. 2) And the geographical positions of the sampling sites were shown in Appendix A Table S3. Choosing 3 to 5 sub-sampling points at each site, the distance between each of these points is less than 1 km. Grab samples were taken from the area surrounding each point (a few square metres) using a small stainless steel shovel. Samples of 1 kg were collected at a depth from 10 to 30 cm at each point and fully pooled in aluminum foil bags (ca. 5000 g each). The samples were cooled in a refrigerator (0°C) during their transport to the laboratory, where they were stored at –20°C until further analysis.

1.2. Simulation of the sediment microenvironment system at different C/N ratios

To activate the soil microorganisms, the sediment microenvironment system was simulated at the laboratory scale. Sediment samples from the three sites were naturally dried, ground and homogenized to powders, sieved through an 80 mesh sieve and subjected to the following procedure: Place 100 g of each sample into a separate 250 mL conical flasks with 10 mL (1 g/L) DBT/dichloromethane solution. Stir to produce even mixing to simulate naturally contaminated sediments, with the total DBT concentration in the sediment at 10 mg/kg. Moisten with sterile distilled water to maintain the proper moisture content after volatilization in the draught cupboard for one night. In this experiment, glycerol and ammonium chloride acted as the carbon source and nitrogen source, respectively, at four different C/N ratios (1:1, 3:1, 5:1 and 9:1). A solvent was added to the cultured sediments with a concentration of ammonium chloride of

30 mmol/L, and these samples were compared with the control group (no extra carbon/nitrogen source). The treated sediments were cultured in the incubator at a constant temperature (20°C), and samples were taken at 0, 4, 7, 10, 14, 20, 28, 36, 45, and 56 days. The samples were stirred every two days, and deionized water was added to maintain the amount of moisture in the sediment.

1.3. DBT quantification

All solvents and reagents were of analytical grade or higher. To determine the concentration of DBT in the cultured sediments, the shock-ultrasonic extraction method was adopted using the following procedure: Take the experimental cultured sediment, which was freeze-dried, ground and homogenized to a fine powder with a mortar and pestle, then sieved through a 500 µm mesh and precisely weighed for extraction (5 g); then, add 5 mL of dichloromethane/isopropanol extraction solvent. Vortex for 30 min to fully mix the extraction solvent and sediment, oscillate for 2 hr on the shaking table, and oscillate for 1 hr in the ultrasonic cleaner. Finally, extract 1 mL of the liquid after centrifugation, and identify it by using gas chromatograph–mass selective (GC–MS) analysis. The recoveries of DBT were 87%–113%.

The concentrations (dry weight) of DBT were determined using an Agilent 7890 GC with a 5973 MS detector (Agilent USA) system equipped with a fused silica capillary DB-5MS column (30 m × 0.25 mm i.d., 0.25 mm film thickness, Agilent, USA). Helium was the carrier gas at a flow of 1 mL/min. The column temperature was programmed from 150°C to 250°C at a rate of 15°C/min. The temperature was first set at 150°C for 2 min and then held for 20 min at 250°C. DBT was analyzed using selective ion monitoring (SIM) mode with an electron impact ionization of 70 eV, an electron multiplier voltage of 1288 eV, and an ion source at 250°C.

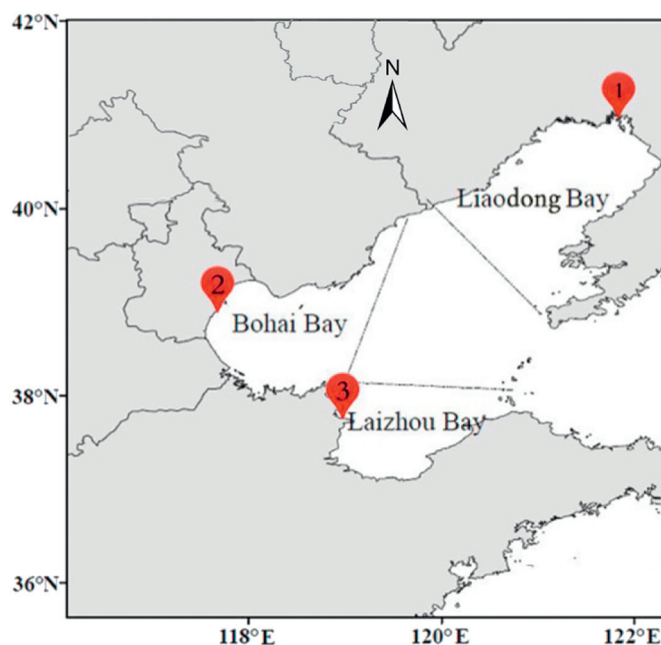


Fig. 2 – Distribution of the sampling sites in the Bohai Rim. 1: Reed wetland of the Liao River estuary; 2: Tidal wetlands of Beida harbor; 3: Estuary wetland of the Yellow River estuary.

1.4. Detection of DBT degradation functional genes

As mentioned earlier, the microbial pathways for the degradation of DBT consist of the Kodama and 4S pathways. For the Kodama pathway, the four enzyme initial dioxygenase, salicylate hydroxylase, 1,2-dioxygenase and catechol 2,3-monooxygenase play very important roles in the entire reaction process. For the 4S pathway, the sulfonate desulfurization enzyme is regarded as a speed-restriction enzyme in the reaction, so it represents the extent of the 4S pathway process. The catalytic genes associated with these enzymes were detected in this study to evaluate the co-relationship between the functional genes and DBT concentrations.

The genes *nahAc*, *nagAc* and *nidA*, the common initial dioxygenase genes encoding the large (α) subunits of dioxygenase, *catA* encoding the catechol-1,2-dioxygenase (Dionisi et al., 2004; Fleming et al., 1993; Debruyne et al., 2007), and *C23O* encoding the catechol 2,3-dioxygenase were quantitatively determined.

The total genomic Deoxyribonucleic acid (DNA) was isolated and purified in triplicate with Soil DNA kits (D5625-01, Omega) from 0.5 g sediment samples. The extracted genomic DNA was detected by 1% agarose gel electrophoresis and stored at -20°C until use. An abundance of bacterial 16S ribosomal genes (16S rRNA), *nidA*, *nahAc*, *nagAc*, *catA*, *C23O* and *dszB* were identified by quantitative PCR (qPCR) on a MyiQ2 Real-Time PCR Detection System (Bio-Rad, USA). The quantification analysis was performed by taking the fluorescence intensity of the SYBR Green dye during amplification; the reaction mixtures contained 10 μL of SYBR Green I PCR master mix (Applied Biosystems), 1 μL of template DNA (sample DNA or plasmid DNA for standard curves), 1 μL of forward primers and reverse primers (Appendix A Table S1), and 7 μL of sterile water. The plasmid DNA used for standard curves was developed as in the procedure reported by Di et al. (2010).

1.5. Data analysis

DBT concentrations were used to calculate the removal efficiencies and degradation rates of DBT at different C/N ratios (1:1, 3:1, 5:1 and 9:1).

The quantitative response relationships between the DBT degradation rates and functional genes were calculated by stepwise regression models using SPSS Statistics 20 (IBM, USA). An a priori p -value of $p < 0.05$ was defined as establishing significant effects. The influence of different functional genes (*nahAc*, *nagAc*, *nidA*, *catA*, *C23O* and *dszB*) on DBT concentrations was derived from path analysis, as described in Wang et al. (2015) and Alwin and Hauser (1975). Direct effects (direct path coefficients) were obtained by the simultaneous solution of the normal equations for multiple linear regression in standard measure. Indirect effects (indirect path coefficients) were derived from simple correlation coefficients between the functional genes using SPSS Statistics 20. The ecological associations between DBT degradation genes were determined by Pearson correlation coefficients using SPSS Statistics 20 (IBM, USA).

The network of functional gene groups and the DBT degradation rate were depicted by Gephi 9.0. The connection coefficients of variation were selected by Pearson correlation analysis at the significance level (P) below 0.05.

2. Results and discussion

2.1. DBT removal performance

The DBT removal efficiency at different C/N ratios is shown in Fig. 3. The results showed that adding glycerol/ammonium chloride at different C/N ratios had an influence on the degradation efficiency of DBT. In the sediments of the three points, the DBT removal efficiency gradually increased with increasing C/N ratio (except for TWS at a C/N ratio = 3). At C/N ratio = 9, the removal efficiencies of DBT at the three points were 13.49%, 15.07% and 33.07% higher than that in the blank group, and the effect of the C/N ratio was the greatest in EWS. Comparing the removal efficiencies of DBT in different wetland sediments at the same C/N ratio, it was found that the degradation performance in EWS was the best. This may be due to the abundance of the 4S pathway genes in EWS being relatively higher than that in RWS and TWS, leading to an intensive 4S process. It was reported that the addition of proper carbon and nitrogen sources could effectively promote the growth and reproduction of bacteria, which was also proven in this study; a high C/N ratio results in the proliferation of bacteria and a high absolute abundance of critical genes, thus leading to the differentiation in the relative abundance, which accounts for the different degradation effects at different sites. Diao (2006) demonstrated that glycerol and ammonium chloride were excellent carbon and nitrogen sources, respectively, for the growth of the 4S-degrading strain MJY_1 at C/N ratio = 3. In this research, the DBT removal efficiency was higher when the C/N ratio increased, which was probably due to the consumption of carbon and nitrogen nutrients by the multitude of bacteria in the soil. Hence, the addition of a carbon source could enhance the effective degradation of DBT.

2.2. DBT removal pathway

2.2.1. Ecological associations

The relationship between the DBT degradative functional genes, which is also regarded as ecological associations, was determined by calculating Pearson correlation coefficients using SPSS Statistics 20 (IBM, USA). Correlation matrices of the Spearman rank correlation coefficients (r) of the three wetlands were developed (Table 1). The 16S rRNA genes were quantified in all samples as a referent for bacterial biomass (Harms et al., 2003).

According to the matrix, the Pearson correlation coefficient between *nagAc* and *catA* reached 0.884 ($p < 0.05$) in RWS because DBT was oxidized with ring opening by the initial dioxygenases (*nagAc*) to salicylate, followed by further degradation through the function of *catA*, which was analogous to the degradation of polycyclic aromatic hydrocarbon (PAHs). The catalysis of *nagAc* and that of *catA* were mutually enhanced (El et al., 2010). In TWS and EWS, the correlation coefficients of *nidA* and *dszB* and of *nidA* and *C23O* were relatively high (0.756 and 0.816, respectively), showing that the catalytic reaction of *nidA* was active. It was reported that *nidA* played an important role in the degradation process of pyrene, benzothiophene and DBT. The bacterial communities

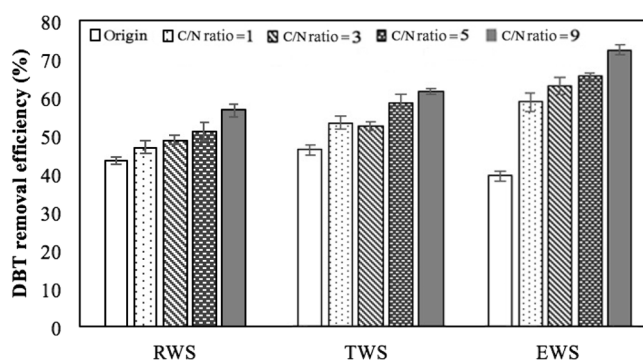


Fig. 3 – DBT removal efficiencies at C/N ratios 1, 3, 5 and 9 for three types of sediment.

associated with *nidA* genes demonstrated a strong adaptability in the PAH-polluted environment due to its catalytic effect on the biodegradation of both lower molecular weight (LMW) PAHs and higher molecular weight (HMW) PAHs (El et al., 2010). Similar to our results, it was reported that the gram-positive bacteria associated with *nidA* genes existed widely in the degradation process of mixtures of phenanthrene, fluorene, anthracene, pyrene, fluoranthene and benzopyrene by wetland sediments in Tianjin, but the *Pseudomonas* associated with the *nahAc* gene was scarcely present (Khan et al., 2001). In addition, the correlations of the abundance of the *dszB* gene, which represented the 4S pathway, with the quantities of the *nidA* gene and the *catA* gene were significant, with coefficients of 0.756 and 0.589, respectively, showing that there were ecological associations to some extent between the Kodama degradation pathway and the 4S desulfurization pathway.

Weak and no significant correlations between concentrations of DBT and quantities of functional genes were found,

which showed that the elimination of DBT was affected by various genes and conditions simultaneously and not determined by one specific functional gene.

2.2.2. Quantitative response relationships

In this study, our objective was to gain quantitative insights into the relative contributions of these functional genes to the DBT degradation rate under different C/N ratio conditions. Therefore, the functional gene group ratios (ratio or summation of different functional genes) were chosen as variables and introduced into stepwise regression analyzes. The results are shown in Table 2. For one site, the key factor related to the DBT degradation rate varied according to the different C/N ratios, which meant that C/N ratio constraints did influence the pathway of DBT degradation. There were smooth discrepancies in functional gene group participation between those of different wetland sediments, and the trend is similar and repeatable.

Table 1 – Pearson correlation coefficients of functional genes in RWS, TWS and EWS ($n = 20$).

	Pearson	16s rRNA	<i>nahAc</i>	<i>nagAc</i>	<i>nidA</i>	<i>catA</i>	C23O	<i>dszB</i>
RWS	16s rRNA	1.000						
	<i>nahAc</i>	−0.044	1.000					
	<i>nagAc</i>	−0.088	0.292	1.000				
	<i>nidA</i>	0.100	−0.272	0.161	1.000			
	<i>catA</i>	−0.080	0.123	0.884**	0.161	1.000		
	C23O	−0.179	0.191	−0.035	−0.303	−0.134	1.000	
	<i>dszB</i>	0.694*	−0.041	−0.142	0.668*	−0.092	−0.178	1.000
TWS	16s rRNA	1.000						
	<i>nahAc</i>	−0.298	1.000					
	<i>nagAc</i>	0.043	−0.200	1.000				
	<i>nidA</i>	0.190	0.084	−0.302	1.000			
	<i>catA</i>	0.435	−0.106	−0.012	−0.269	1.000		
	C23O	−0.115	−0.174	0.140	−0.144	0.445*	1.000	
	<i>dszB</i>	0.793*	−0.204	−0.269	0.756**	0.182	−0.232	1.000
EWS	16s rRNA	1.000						
	<i>nahAc</i>	0.370	1.000					
	<i>nagAc</i>	0.402*	0.260	1.000				
	<i>nidA</i>	−0.035	0.233	−0.041	1.000			
	<i>catA</i>	0.509*	0.231	0.199	0.170	1.000		
	C23O	0.102	0.248	0.575*	0.816**	0.146	1.000	
	<i>dszB</i>	0.536*	0.390	0.215	0.205	0.589**	0.326	1.000

RWS: reed wetland sediments, TWS: tidal wetlands sediments, EWS: estuary wetland sediments.

** Statistically significant ($p < 0.01$, two-sided test);

* Statistically significant ($p < 0.05$, two-sided test).

Table 2 – Quantitative response relationships between nitrogen transformation rates and functional gene groups in RWS, TWS, and EWS.

Wetland type	C/N ratio	Stepwise regression equations	R ²	N	P
RWS	1:1	$V_{\text{DBT}} \text{ (ng/day)} = 0.059 + 0.475(\text{nahAc} + \text{nagAc})/\text{C23O}$	0.972	5	0.002
	3:1	$V_{\text{DBT}} \text{ (ng/day)} = 0.014 + 0.033(\text{nahAc} + \text{nagAc} + \text{nidA})/(\text{catA} + \text{C23O})$	0.864	5	0.022
	5:1	$V_{\text{DBT}} \text{ (ng/day)} = 0.071 + 1.500 \times 10^{-4} \text{ nagAc/dszB}$	0.960	5	0.005
	9:1	$V_{\text{DBT}} \text{ (ng/day)} = 0.040 + 4.147 \times 10^{-5} \text{ nidA/dszB}$	0.810	5	0.041
	Total	$V_{\text{DBT}} \text{ (ng/day)} = 0.087 + 0.069 \text{ nagAc/catA}$	0.341	20	0.028
TWS	1:1	$V_{\text{DBT}} \text{ (ng/day)} = 0.054 + 109.672 \times \text{C23O}/16\text{S}$	0.776	5	0.048
	3:1	$V_{\text{DBT}} \text{ (ng/day)} = 0.082 + 0.024(\text{nahAc} + \text{nagAc})/(\text{catA} + \text{C23O})$	0.883	5	0.018
	5:1	$V_{\text{DBT}} \text{ (ng/day)} = 0.008 + 0.003 \times \text{nagAc/dszB}$	0.919	5	0.010
	9:1	$V_{\text{DBT}} \text{ (ng/day)} = 0.196 + 4.891 \times 10^{-5} \text{ nidA/dszB}$	0.906	5	0.013
	Total	$V_{\text{DBT}} \text{ (ng/day)} = 0.106 + 0.003 \text{ nahAc/catA}$	0.390	20	0.003
EWS	1:1	$V_{\text{DBT}} \text{ (ng/day)} = 0.127 - 7.588(\text{catA} + \text{C23O})/16\text{S}$	0.836	5	0.030
	3:1	$V_{\text{DBT}} \text{ (ng/day)} = 0.051 + 0.043(\text{nahAc} + \text{nagAc})/\text{C23O}$	0.974	5	0.002
	5:1	$V_{\text{DBT}} \text{ (ng/day)} = 0.080 + 0.002 (\text{nagAc} + \text{nagAc})/\text{dszB}$	0.898	5	0.014
	9:1	$V_{\text{DBT}} \text{ (ng/day)} = 0.092 + 446.619 \text{ dszB}/16\text{S}$	0.926	5	0.009
	Total	$V_{\text{DBT}} \text{ (ng/day)} = 0.085 + 50.705 (\text{nahAc} + \text{nagAc})/\text{dszB}$	0.474	20	0.001

In RWS, the degradation rate of DBT was determined by $(\text{nahAc} + \text{nagAc})/\text{C23O}$, $(\text{nahAc} + \text{nagAc} + \text{nidA})/(\text{catA} + \text{C23O})$, nagAc/dszB , and nidA/dszB at C/N ratios of 1, 3, 5 and 9. When the C/N ratio was relatively low (C/N ratio = 1), $(\text{nahAc} + \text{nagAc})/\text{C23O}$ was the key factor, showing a positive relationship with the DBT degradation rate. The *nahAc* and *nagAc* genes are often regarded as reaction markers for the conversion of DBT to dihydroglycol products. The catechol 2,3-dioxygenase gene (encoded by C23O) was the critical enzyme that catalyzed salicylate to tricarboxylic acid and then to water and CO₂. The *nahAc*, *nagAc* and C23O genes were involved in the two consecutive steps of the Kodama pathway. Their cooperation indicated that the Kodama pathway is the dominant reaction at a low C/N ratio. When the C/N ratio increases to 3, $(\text{nahAc} + \text{nagAc} + \text{nidA})/(\text{catA} + \text{C23O})$ was the primary factor. The *nidA* gene is also responsible for the reaction of the dihydroglycol products into salicylate in the upper Kodama pathway. The *catA* gene, another gene representing a Kodama downstream process, participated in the formula, showing that the entire Kodama pathway contributed to the DBT degradation rate. With continuous addition of glycerol to maintain a C/N ratio of 5, *nagAc/dszB* became the determining factor related to the degradation rate. The *dszB* gene is regarded as the marker gene for the 4S pathway, indicating that the 4S pathway has occurred in the reaction. When the C/N ratio increased to 9, *nidA/dszB* was the primary factor, meaning that the 4S pathway jointly determined the degradation rate with the Kodama pathway. Nakayama et al. (2002) had reported that the further degradation of 2-hydroxybiphenyl, a desulfurization product of the 4S upper pathway, required the participation of Kodama pathway-related genes for the ring cleavage, which could explain the cooperation of the two pathways at a high C/N ratio.

There were very few differences between the results of RWS and TWS. When the C/N ratio was 1, C23O/16S was the dominant factor, showing a positive relationship with the DBT degradation rate. The C23O gene is the typical gene of the Kodama upper pathway. In addition, $(\text{nahAc} + \text{nagAc})/(\text{catA} + \text{C23O})$ was responsible for the degradation rates at a C/N ratio

of 3, showing that the entire Kodama pathway contributed to the DBT degradation rate. When the C/N ratio was increased to 5 and 9, *nagAc/dszB* and *nidA/dszB* played key roles in the reaction, respectively, with the same results being obtained as for RWS, indicating that the 4S pathway began to react in the entire process. We concluded that both the Kodama pathway and the 4S pathway commonly affected the DBT degradation at higher C/N ratios. In RWS and TWS, a C/N ratio of 3 was the most suitable condition for the Kodama pathway and the expression of the relevant functional genes. Two formulas based on the entire data set also revealed that the Kodama genes were responsible for the DBT degradation rate, indicating that the Kodama pathway was the critical process from a larger perspective, despite the 4S pathway occurring when the C/N ratio increased to 5.

In EWS, the shifts of functional genes groups differed from those in RWS and TWS, revealing that the degradation process was different. At a C/N ratio of 1, $(\text{catA} + \text{C23O})/16\text{S}$ was the dominant factor, showing that only Kodama downstream-pathway genes had a positive contribution to the DBT degradation rate, with no Kodama upper-pathway genes occurring in the formula. With the increase in the C/N ratio, the Kodama upper-pathway genes accompanied by the downstream-pathway gene, $(\text{nahAc} + \text{nagAc})/\text{C23O}$, became the key factor, indicating that the complete Kodama pathway controlled the degradation process. When the C/N ratio was 5, the 4S pathway began to dominate the DBT degradation rate. Kodama pathway genes disappeared when the C/N ratio was 9, and *dszB/16S* was the key factor, showing a positive relationship with the DBT degradation rate. Only the 4S pathway participated in the reaction, and the Kodama pathway contributed very little according to the formula. The *nidA* gene did not appear as it did in RWS and TWS.

According to the analyses above, we concluded that the C/N ratio has obvious impacts on the DBT degradation rate. At a low C/N ratio, Kodama genes played the key role in the reaction, and the Kodama pathway mainly determined the degradation rate. At a high C/N ratio (up to 5), the 4S gene *dszB* appeared, revealing that the 4S pathway gained a positive relationship with the DBT degradation rate. Three experiments on three wetland

sediments jointly confirmed this transformation rule. Aggarwal et al. (2010) had revealed that 4 mol NADH was necessary for the transformation of 1 mol DBT into 2-HBP in the process of the 4S pathway and that other nicotinamide adenine dinucleotide (NADH)-dependent activities were inhibited at same time, which meant that the DBT degradation rate would decline without the addition of an extra energy source. Yan et al. had studied the utilization of different carbon sources for *Rhodococcus erythropolis* to evaluate their effects on the accumulation of NADH. Glycerol was proven to be the NADH source that stimulated microorganism growth and DBT biodegradation (Yan et al., 2000). This agrees with the result in our research.

2.2.3. DBT degradation pathways transformation

To determine the contribution of functional gene groups to DBT degradation in RWS, TWS, and EWS, path analysis was used in this study. The positive or negative values of the effects indicated the functional gene groups that contributed to the growth or reduction in the DBT degradation rate (Pang et al., 2015).

A higher direct effect of $(nahAc + nagAc)/C23O$ (0.722) on the DBT degradation rate compared with $(nahAc + nagAc + nidA)/(catA + C23O)$ (−0.251), $nagAc/dszB$ (0.279), and $nidA/dszB$ (−0.137) was observed under the C/N ratio of 1 in RWS (Fig. 4a). With the growth of the C/N ratio, $(nahAc + nagAc + nidA)/(catA + C23O)$, $nagAc/dszB$, and $nidA/dszB$ became the main factor for the contribution to the degradation rate in turn, and their direct effects increased to 0.930 (C/N ratio = 3), 0.822 (C/N ratio = 5), and 0.877 (C/N ratio = 9). These results suggested that the change in the C/N ratio clearly impacted the reaction process and that the DBT degradation pathway shifted from the single Kodama effect to the cooperation of the Kodama and 4S pathways, just as we have discussed in Section 2.2.2. In TWS, the results further supported this point (Fig. 4b). At C/N ratios of 1, 3, 5 and 9, $C23O/16S$, $(nahAc + nagAc)/(catA + C23O)$, $nagAc/dszB$ and $nidA/dszB$ were the main factors in the DBT degradation rate, and their effects were 0.881, 0.940, 0.923 and 0.652, respectively. In RWS and TWS, the effects of the 4S pathway-related gene groups such as $nagAc/dszB$ and $nidA/dszB$ were relatively low compared with the effects of the Kodama-related gene groups, revealing that the 4S pathway existed but was not the dominant degradation gene influencing the rate. The Kodama pathway was more specialized and was the critical degradation step for the elimination of DBT. It was reported that the wild-type 4S pathway degrading bacteria isolated from the natural environment cannot metabolize dodecane, n-hexadecane and naphthalene as carbon sources (Caro et al., 2007), which shows that the 4S-pathway desulfurizing bacteria did not occupy the same dominant position in the biodegradation of DBT compared with the Kodama pathway bacteria. In most of the wetland sediments, the Kodama-pathway bacteria played a more significant role in the degradation of DBT due to their ability to metabolize carbon. This conclusion agreed with the formula shown in Table 2.

The transformation of the main factors in EWS was different (Fig. 4c); $(catA + C23O)/16S$, $(nahAc + nagAc)/C23O$ and $(nahAc + nagAc)/dszB$ became the dominant factors contributing to the DBT degradation rate at the C/N ratio of 1, 3 and 5, and their direct effects were −0.915, 0.967 and 0.707, respectively. It was noted that a single 4S pathway-related

gene group, $dszB/16S$, was the main factor accounting for the rate at the C/N ratio of 9 (direct effect = 0.954). Its direct effect was above the average all the time, indicating that the contribution of the 4S pathway is relatively high. In addition, the effect of the Kodama downstream-pathway gene group, $(catA + C23O)/16S$, was negative, showing that there may be a competition relationship between the Kodama pathway and the 4S pathway in EWS. $C23O$ and $catA$ have the ability to cleave the rings of pyrocatechol at the ortho and meta positions, which is an oxygen consumption process. It is further reported that oxygen was required for the oxidation of C–S in the 4S upper pathway (Singleton et al., 2009). Therefore, the bacterial communities associated with the 4S pathway-related genes had advantages in their competition with those associated with the Kodama pathway genes in EWS, and the two pathways inhibited each other to some extent.

2.3. Correlation network analysis of functional gene groups and the DBT degradation rate

For the comprehensive understanding of the functional gene groups and DBT degradation rate under different C/N ratio constraints, network analysis was introduced in this study. The absolute abundance of a single gene could indicate the potential of various microbial ecological processes, while the functional genome (the ratio of the absolute abundances of different genes) could show the potential relative contribution to different ecological processes. In this sense, ecological network analysis was conducted to investigate the relation between 37 special DBT-degrading genomes and the DBT degradation rate. Thirty-seven DBT-degrading functional genomes and their corresponding meanings were described in Appendix A Table S2.

The RWS network diagram under various conditions (C/N ratio = 1, 3, 5 and 9) is shown in Appendix A Fig. S1. At C/N ratio = 1, a large group mainly related to the Kodama genome, $nahAc$ and $nagAc$ was present in the network diagram, which apparently demonstrated that the degradation rate was solely related to this group. This large group had a crucial effect in the system as the rate-limiting factor in the DBT degradation process. At C/N ratio = 3, the RWS network diagram was not compact and was divided into 3 parts. The upper and lower groups were aggregates of functional genes upstream and downstream of the Kodama pathway, implying a coupling between the upstream and downstream of the Kodama process, which was related to the degradation rate. The right group was $nidA$ and $dszB$, mainly of the 4S pathways, which did not perform as the rate-limiting factor of the reaction. At C/N ratio = 5, the $dszB$ gene of the 4S pathway frequently appeared in the right group of the network diagram, related to the degradation rate, which proved the coupling of the 4S pathway and the DBT degradation process. Hence, the 4S pathway began to have an effect on degradation when the C/N ratio increased to 5. At C/N ratio = 9, the large groups in the network diagram mainly involved the upstream gene of the Kodama pathway and the functional gene $dszB$ of the 4S pathway, where $nidA$ and $dszB$ occurred frequently; the downstream genes ($catA$ and $C23O$) were scattered and exhibited no sufficient coupling. It should be noted that the relationship between the degradation rate and the major groups was quite low.

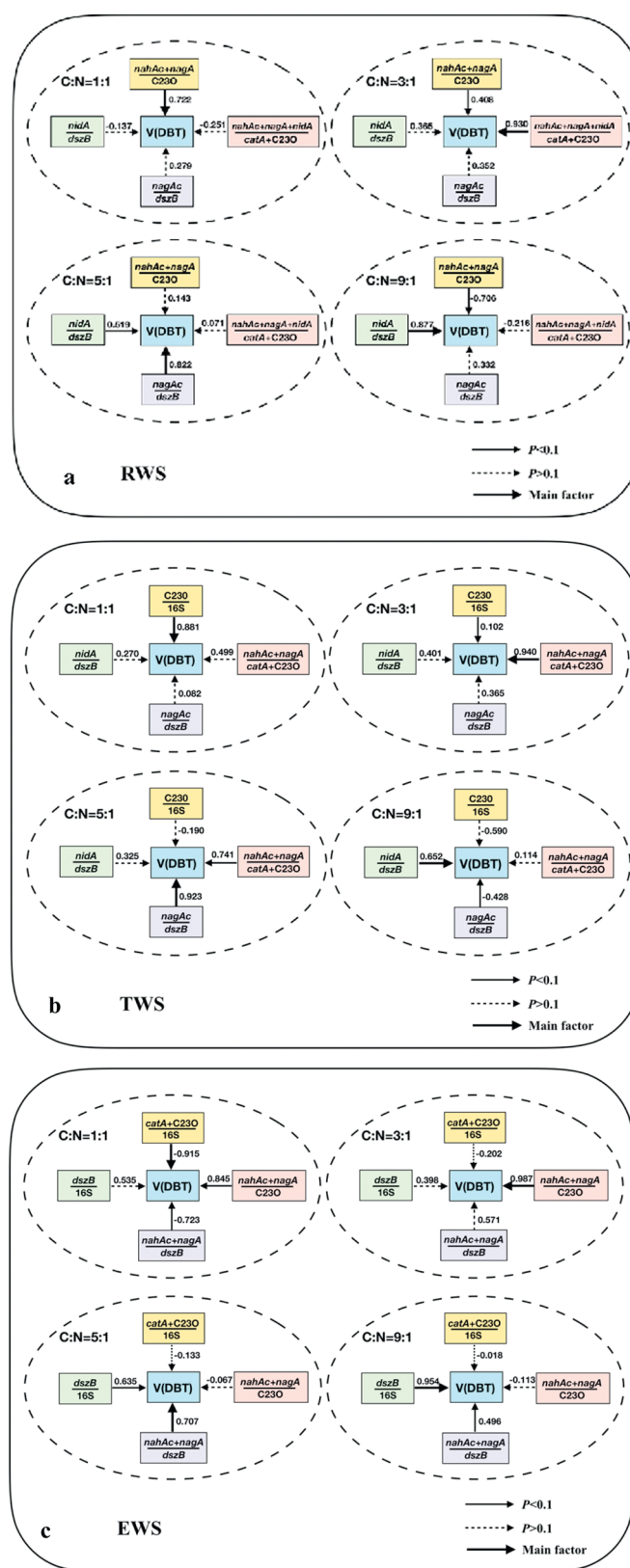


Fig. 4 – Path diagrams assessing the effects of functional gene groups on the DBT degradation rate at different C/N ratios. (a) Reed wetland sediments; (b) Tidal wetlands sediments; (c) Estuary wetland sediments.

The network diagram for TWS is shown in Appendix A Fig. S1. At a C/N ratio of 1, a large group mainly containing the Kodama pathway upstream genes was connected firmly but not regarded as the rate-limiting factor in DBT degradation since these genes had little relationship with the degradation rate. The Kodama downstream gene C230 groups connected directly with the rate, implying that they were the rate-limiting factor for the reaction despite a low connectivity. The gene *dszB* of the 4S pathway is not systematic in the network diagram. When C/N ratio = 3, there are two main groups. The upper part showed that the coupling between the upstream and downstream of the Kodama gene groups was related to the degradation rate and was regarded as the rate-limiting factor. The 4S pathway-related gene groups were involved in the lower part, indicating that the 4S pathway had participated in the reaction with the increase in the C/N ratio. At a C/N ratio of 5, the connectivity of the functional gene group network diagram was not strong, but the rate was linked to the 4S pathway gene groups. In contrast, at a C/N ratio of 9, the *dszB* gene in the *nidA* gene groups jointly determined the degradation rate and indicated that the Kodama and 4S pathways collaborated in the reaction.

The EWS network diagram (Appendix A Fig. S1) exhibited a similar phenomenon but with fewer modularity effects compared with those of RWS and TWS. When C/N ratio = 1 and 3, the rate was mainly connected with the Kodama-related gene groups, showing that the Kodama pathway was the dominant factor in the reaction. When the C/N ratio increased to 5, the connectivity of the *dszB* groups became high, and the 4S pathway occurred. At a C/N ratio of 9, the connectivity of the entire network diagram was relatively low, and the distribution of gene groups was dispersed. The *dszB* groups were integrated with rate and regarded as the rate-limiting factor of the reaction.

The ecological networks further proved the relationship between the C/N ratio and the expression of functional genes. At a low C/N ratio, the Kodama-related genes integrated as a large group and connected with the degradation rate, indicating that the Kodama pathway contributed more to the entire reaction. When the C/N ratio increased, the groups of the 4S pathway marker gene *dszB* assembled with great connectivity, and the 4S pathway played an important role in the degradation process.

3. Conclusions

The present research investigated the quantitative response of the biodegradation rate of DBT to relative functional genes in coastal sediments by the Kodama and 4S pathways. We found that the C/N ratio had obvious impacts on the DBT degradation reaction for both the Kodama and 4S pathways, especially in estuary wetland sediments. For every sediment, it was observed that the Kodama pathway mainly contributed to DBT degradation at low C/N ratios, with stronger expression of the Kodama-related functional genes. When the C/N ratio increased to 5, the 4S pathway process occurred, and the collaboration of the two pathways became the main factor, indicating a shift in pathway from the Kodama pathway to the 4S pathway. Compared with reed wetland sediments and tidal

wetland sediments, the 4S pathway-related bacteria were more active in the estuary wetland sediments and took a dominant position at a high C/N ratio. There was competition between the two types of pathways, and it was clear that the estuary wetland sediment environments were more suitable for the proliferation of 4S pathway-related bacteria, which was also proven by their high relative abundance. The higher degradation efficiency of EWS indicated the greater participation of the 4S pathway in the DBT biodegradation reaction. Low accumulation of 2-hydroxybiphenyl in reed wetland sediments and tidal wetland sediments also proved the ability of complete metabolizing of DBT of Kodama pathway.

Acknowledgments

The Foundation for Innovative Research Groups of the National Natural Science Foundation of China (No. 51721006) and the National Natural Science Foundation of China (No. 51679001) provided support for this study.

Appendix A. Supplementary data

Supplementary data to this article can be found online at <https://doi.org/10.1016/j.jes.2018.04.029>.

REFERENCES

- Abbasian, F., Lockington, R., Megharaj, M., Naidu, R., 2016. Identification of a new operon involved in desulfurization of dibenzothiophenes using a metagenomic study and cloning and functional analysis of the genes. *Enzym. Microb. Technol.* 87–88, 24–28.
- Aggarwal, S., Karimi, I.A., Dong, Y.L., 2010. Flux-based analysis of sulfur metabolism in desulfurizing strains of *Rhodococcus erythropolis*. *FEMS Microbiol. Lett.* 315 (2), 115–121.
- Alwin, D.F., Hauser, R.M., 1975. The decomposition of effects in path analysis. *Am. Sociol. Rev.* 40, 37–47.
- Caro, A., Boltos, K., Letón, P., García-Calvo, E., 2007. Dibenzothiophene biodesulfurization in resting cell conditions by aerobic bacteria. *Biochem. Eng. J.* 35 (2), 191–197.
- Cheng, L., Zhaoyin, W., 2003. Analysis on Water Quality of the Estuary around Bohai Bay. *Environ. Pollut. Control.* 25 (4), 222–225.
- Debruyne, J.M., Chewning, C.S., Sayler, G.S., 2007. Comparative quantitative prevalence of mycobacteria and functionally abundant *nidA*, *nahAc*, and *nagAc* dioxygenase genes in coal tar contaminated sediments. *Environ. Sci. Technol.* 41 (15), 5426–5432.
- Di, H.J., Cameron, K.C., Shen, J.P., Winefield, C.S., O'Callaghan, M., Bowatte, S., et al., 2010. Ammonia-oxidizing bacteria and archaea grow under contrasting soil nitrogen conditions. *FEMS Microbiol. Ecol.* 72 (3), 386–394.
- Diao, J.Z., 2006. The Study on Culturing Strain of Desulfurizative Enzyme to Dibenzothiophene and Partial Characters of the Enzyme. Doctoral dissertation. Sichuan University, China.
- Diao, S., Wang, H.Q., Xu, J., Zhao, Y.C., 2017. Isolation, identification and analysis of degradation ability of a cold-resistant haloduric pyrene-degrading strains. *China Environ. Sci.* 37 (2), 677–685.
- Dionisi, H.M., Chewning, C.S., Morgan, K.H., Menn, F.-M., Easter, J.P., Sayler, G.S., 2004. Abundance of dioxygenase genes similar to

- Ralstonia* sp. strain U2 *nagAc* is correlated with naphthalene concentrations in coal tar-contaminated freshwater sediments. *Appl. Environ. Microbiol.* 70 (7), 3988.
- El, A.N., Deverslamrani, M., Chatagnier, G., Rouard, N., Martinlaurent, F., 2010. Molecular analysis of the catechol-degrading bacterial community in a coal wasteland heavily contaminated with PAHs. *J. Hazard. Mater.* 177 (1–3), 593–601.
- Fleming, J.T., Sanseverino, J., Sayler, G.S., 1993. Quantitative relationship between naphthalene catabolic gene-frequency and expression in predicting PAH degradation in soils at town gas manufacturing sites. *Environ. Sci. Technol.* 27 (6), 1068–1074.
- Harms, G., Layton, A.C., Dionisi, H.M., Gregory, I.R., Garrett, V.M., Hawkins, S.A., et al., 2003. Real-time PCR quantification of nitrifying bacteria in a municipal wastewater treatment plant. *Environ. Sci. Technol.* 37 (2), 343–351.
- Hu, N., Shi, X., Liu, J., Huang, P., Liu, Y., Liu, Y., 2010. Concentrations and possible sources of PAHs in sediments from Bohai Bay and adjacent shelf. *Environ. Earth Sci.* 60 (8), 1771–1782.
- Hu, B., Li, J., Zhao, J., Yang, J., Bai, F., Dou, Y., 2013. Heavy metal in surface sediments of the Liaodong Bay, Bohai Sea: distribution, contamination, and sources. *Environ. Monit. Assess.* 185 (6), 5071–5083.
- Huang, L., Xie, J., Shi, X.F., Lian, J.Y., 2013. Research on the isolation, identification and degradation characteristics of a diesel oil degrading strain. *Adv. Mater. Res.* 641–642 (1), 206–210.
- Jiao, W., Wang, T., Lu, Y., Chen, W., He, Y., 2014. Ecological risks of polycyclic aromatic hydrocarbons found in coastal sediments along the northern shores of the Bohai Sea (China). *Chem. Ecol.* 30 (6), 501–512.
- Jie, L.I., Zhang, W., Xin, J., Jianlin, B.I., Shou, Y., Shan, B., 2015. Detection of phosphorus components in the soils of coastal wetlands surrounding Bohai Sea. *Acta Sci. Circumst.* 35 (4), 1143–1151.
- Kaufman, E.N., Harkins, J.B., Borole, A.P., 1998. Comparison of batchstirred and electrospray reactors for biodesulfurization of dibenzothiophene in crude oil and hydrocarbon feedstocks. *Appl. Biochem. Biotechnol.* 73 (2–3), 127–144.
- Khan, A.A., Wang, R.F., Cao, W.W., Doerge, D.R., Wennerstrom, D., Cerniglia, C.E., 2001. Molecular cloning, nucleotide sequence, and expression of genes encoding a polycyclic aromatic ring dioxygenase from *Mycobacterium* sp. strain PYR-1. *Appl. Environ. Microbiol.* 67 (8), 3577.
- Kodama, K., 2008. Co-metabolism of dibenzothiophene by *Pseudomonas jianii*. *J. Agric. Chem. Soc. Jpn.* 41 (7), 1305–1306.
- Kodama, K., Umehara, K., Shimizu, K., Nakatani, S., Minoda, Y., Yamada, K., 1973. Identification of microbial products from dibenzothiophene and its proposed oxidation pathway. *J. Agric. Chem. Soc. Jpn.* 37 (1), 45–50.
- Li, G., Xia, X., Yang, Z., Wang, R., Voulvoulis, N., 2006. Distribution and sources of polycyclic aromatic hydrocarbons in the middle and lower reaches of the Yellow River, China. *Environ. Pollut.* 144 (3), 985–993.
- Li, G.Q., Li, S.S., Zhang, M.L., Wang, J., Zhu, L., Liang, F.L., et al., 2008. Genetic rearrangement strategy for optimizing the dibenzothiophene biodesulfurization pathway in *Rhodococcus erythropolis*. *Appl. Environ. Microbiol.* 74 (4), 971–976.
- Li, L., Zhao, C., Liu, Q., Zhang, Y., Liu, C., Xue, J., 2014. Optimization for microbial degradation of dibenzothiophene by *pseudomonas* sp. lky-5 using response surface methodology. *China Pet. Process. Petrochem. Technol.* 16 (1), 19–26.
- Liu, D., Zhu, L., 2014. Assessing China's legislation on compensation for marine ecological damage: a case study of the Bohai oil spill*. *Mar. Policy* 50 (1), 18–26.
- Nakayama, N., Matsubara, T.T., Moroto, Y., Kawata, Y., Koizumi, K., Hirakawa, Y., et al., 2002. A novel enzyme, 2'-hydroxybiphenyl-2-sulfinate desulfinate (DszB), from a dibenzothiophene-desulfurizing bacterium *Rhodococcus erythropolis* KA2-5-1: gene overexpression and enzyme characterization. *Biochim. Biophys. Acta* 1598 (2), 122–130.
- Oldfield, C., Pogrebinsky, O., Simmonds, J., Olson, E.S., Kulpa, C.F., 1997. Elucidation of the metabolic pathway for dibenzothiophene desulfurization by *Rhodococcus* sp. strain IGTS8 (ATCC 53968). *Microbiology* 143 (9), 2961–2973.
- Pang, Y., Zhang, Y., Yan, X., Ji, G., 2015. Cold temperature effects on long-term nitrogen transformation pathway in a tidal flow constructed wetland. *Environ. Sci. Technol.* 49 (22), 13550–13557.
- Seo, J.S., Keum, Y.S., Li, Q.X., 2009. Bacterial degradation of aromatic compounds. *Int. J. Environ. Res. Public Health* 6 (1), 278.
- Singleton, D.R., Ramirez, L.G., Aitken, M.D., 2009. Characterization of a polycyclic aromatic hydrocarbon degradation gene cluster in a Phenanthrene-degrading *Acidovorax* strain. *Appl. Environ. Microbiol.* 75 (9), 2613.
- Wang, H., Ji, G., Bai, X., He, C., 2015. Assessing nitrogen transformation processes in a trickling filter under hydraulic loading rate constraints using nitrogen functional gene abundances. *Bioresour. Technol.* 177 (177C), 217–223.
- Xin, J., Tian, W., Liu, Q., Qiao, K., Jing, Z., Gong, X., 2017. Biodegradation of the benzo[a]pyrene-contaminated sediment of the Jiaozhou Bay wetland using *Pseudomonas* sp. immobilization. *Mar. Pollut. Bull.* 117 (1–2), 283.
- Yan, H., Kishimoto, M., Omasa, T., Katakura, Y., Suga, K., Okumura, K., et al., 2000. Increase in desulfurization activity of *Rhodococcus erythropolis* KA2-5-1 using ethanol feeding. *J. Biosci. Bioeng.* 89 (4), 361.